Designing and Testing a New Microcantilever Calibration Device for an Advanced Atomic Force Microscope

Qizhan Tam (University of Pennsylvania, Mechanical Engineering), *Littlejohn Fellow*

Xin-Z. Liu, Professor Robert. W. Carpick, Mechanical Engineering and Applied Mechanics

***Abstract*— Lateral force calibration of Atomic Force Microscopes (AFMs) is used to convert lateral force signals in volts to newtons by finding the lateral force calibration constant. For the RHK ultra-high vacuum (UHV) 750 AFM model produced by RHK Technology, the lateral force calibration methods currently used are the beam geometry and wedge methods. The beam geometry method is based on an idealized model of the cantilever beam which is used to sense forces during scanning of specimens. This exposes the method to large errors as cantilevers may have varying dimensions. The wedge method is more accurate but it damages the cantilever tip and it is difficult to use for this AFM model. The Diamagnetic Lateral Force Calibrator (D-LFC) has none of these drawbacks. It is based entirely on empirical data and no foreknowledge of cantilever properties is required. A key component of the D-LFC is the Diamagnetic Levitation Spring System (DLSS), which is an arrangement of four magnets with a graphite-mica sheet levitating on top. The spring constant of the DLSS is found by tracking the motion of the graphite-mica sheet's oscillation. The DLSS is placed in the UHV chamber and scanned laterally, obtaining a linear relationship between the lateral voltage signal and the lateral displacement of the graphite-mica sheet. However, custom AFM parts are required to be designed and produced for the alignment between the cantilever and DLSS. The DLSS's spring constant is then multiplied to the lateral displacement, leading to a lateral voltage signal vs. lateral force relationship. The lateral force constant is established by taking the inverse slope of the plot. Finally, we show the comparison between the beam geometry and D-LFC methods using the same cantilever.**

***Index Terms*—Diamagnetic Force Lateral Calibration (D-FLC), Diamagnetic Levitation Spring System (DLSS), DLSS stiffness, graphite-mica sheet, lateral force constant, Ultra High Vacuum (UHV)**

I. Introduction

Atomic Force Microscopes (AFM) function by having a laser beam reflecting off the surface of a cantilever onto a photosensitive diode (fig. 1). The cantilever tip interacts with the specimen's surface, causing it to deflect. This changes the beam's position on the photosensitive diode which is then translated into voltage signal. Different properties of the specimen can be measured and analyzed this way. The property that we are interested in this paper, friction, is measured when the tip experiences lateral force while scanning, causing the cantilever to undergo torsional deflection (fig. 2). This results in the laser beam deflecting laterally on the photosensitive diodes which is translated into voltage signals.

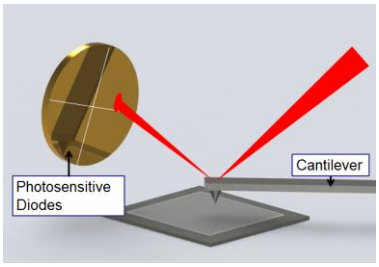

Figure 1: Simple AFM depiction.

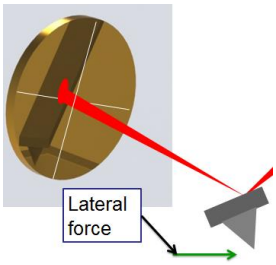

Figure 2: Lateral deflection.

Lateral force calibration is required to determine the lateral force constant, α, which converts lateral voltage signal to lateral force in newtons. Usage of the RHK UHV 750 AFM currently relies on the optical beam geometry method and the wedge calibration method for lateral force calibration. The beam geometry method (Appendix) is based on an idealized model of cantilevers and the AFM's photosensitive diode, potentially resulting in large errors. The wedge calibration depends on empirical data, and hence is more reliable. However, the RHK "Beetle" scan head of the AFM has a limited height vertical displacement, causing great difficulties in using this method. Wedge calibration also requires large pressures to be exerted by the tip on the wedge surface, potentially damaging the tip during the calibration process.

D-LFC does not have any of the above drawbacks. Similar to the wedge calibration method, D-LFC relies on empirical data and does not require foreknowledge of cantilever properties [2]. There is also minimum wear of the cantilever tip as the method only requires the tip to twist at an angle instead of scrape against a surface.

A critical component used in D-LFC is the Diamagnetic Levitation Spring System (DLSS). In this project, the DLSS consists of a graphite sheet with mica attached to the top which is then levitated on top of a set of four magnets (fig. 3). Once the DLSS is pre-calibrated (to be discussed Section 3), it is used in D-LFC by scanning along a diagonal axis of the graphite-mica sheet with a cantilever tip. As the graphite-mica sheet is displaced further from its equilibrium center, the restoring force increases proportionately (fig. 4).

One of the key procedures required for the D-LFC method

is the alignment of the cantilever along one of the two diagonal axes of the graphite-mica sheet. The RHK UHV AFM has a unique Beetle scan head which rotates when the tip approaches the specimen (fig. 5). This results in the alignment of the cantilever along an axis of the setup to be nearly impossible. Positioning of the D-LFC setup is also risky as access to and manipulating inside the chamber is limited to a metal fork. The graphite-mica sheets regularly fall out of position whenever the D-LFC setup is moved within the UHV chamber.

A previous postdoctoral researcher, Dr. Qunyang Li, had worked on the D-LFC method on the RHK 350 AFM. A simple custom specimen holder was made to enable the rotation of the specimen. Slots were cut in place of the screw holes and the specimen holder was made out of steel. However, as the custom holder is still clamped between other parts, the rotation of the holder is directly dependent on how tightly the custom holder was clamped. Hence, in order to adjust the orientation of the magnets, the entire assembly has to be removed from the chamber or by loosening the screws and coarsely rotating the magnets. This compromises the mechanical stability of the setup. As the setup was made from steel, the magnets were also very difficult to remove. The magnets were inevitably damaged whenever there were attempts to remove them from the setup. The setup also did not solve the risk of the graphite-mica sheet falling from the custom holder.

There are three major objectives in this project. The first objective is to calibrate DLSSs for use in D-LFC. The second objective is to design and manufacture new custom AFM sample holder parts which will solve the usability issues of D-LFC. The third objective is to use D-LFC in the RHK UHV 750 AFM and determine its suitability for experimental applications.

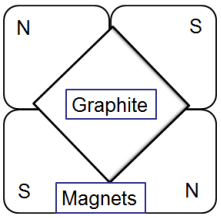

Figure 3: DLSS setup diagram.

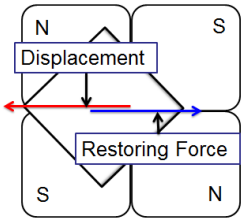

Figure 4: How DLSS works.

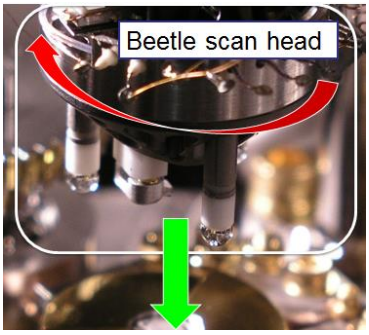

Figure 5: Beetle scan head lowers by rotating.

II. Background

A. *Finding the DLSS spring constant.*

Based on the paper written by the developers of the D-LFC method, Li et al., there are three steps in calibrating the lateral force constant of each cantilever for AFMs. First, the **spring constant**, $\boldsymbol{k}$, of the DLSS needs to be found. This is achieved by fitting the displacement of the graphite-mica sheets to a viscous damping model: $x_1(t) = e^{-\zeta\omega_n t}(a_1 \sin \omega_d t + a_2 cos\ \omega_d t)$ [3], where $x_1(t)$ represents the displacement of the graphite-mica sheet along an axis with respect to time, t; ζ is the damping ratio; ω_n is the undamped angular frequency (i.e. natural resonant frequency); ω_d is the damped angular frequency (i.e. natural damped frequency) of the oscillation. To simplify the plot fitting process, the following relationship may be used: $\omega_d = \omega_n\sqrt{1-\zeta^2}$ [3]. The DLSS spring constant is then calculated with the equation: $k = m\omega_n^2 = m\omega_d^2/(1-\zeta^2)$. [3]

B. *Finding the lateral optical sensitivity.*

The **lateral optical sensitivity**, $\boldsymbol{s_l}$, is the ratio of the graphite's displacement and the photosensitive diode's lateral voltage signal. In other words, the linear relationship between the displacement of the graphite-mica sheet, Δx, and the lateral voltage signal, V, needs to be found.

C. *Calculating the lateral force constant.*

The lateral force is calculated from $f = \Delta x * k$. The **lateral force constant**, $\boldsymbol{\alpha}$, can then be found by using the following equation: $\alpha = f/V$. [3]

III. Pre-calibrating DLSS

A. *Preparation of DLSS*

Mica sheets were attached to square graphite sheets of ~5×5×0.5 mm^2 (length × width × thickness) with vacuum-compatible glue (fig. 6). They were then heated for the glue to cure. The mean of multiple readings from a microbalance was used to determine the mass of the mica-graphite sheets. Neodymium magnets were then arranged in alternating magnetic poles in a square shape. A graphite-mica sheet was placed on top of each magnet set (fig. 7).

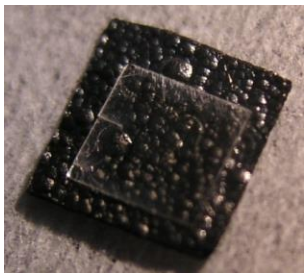
Figure 6: Graphite-mica sheet.

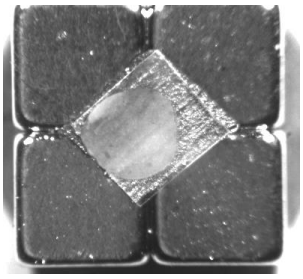
Figure 7: DLSS.

B. *High speed motion capture of DLSS*

A high speed camera was used to capture the motion of the diamagnetic levitation spring systems which were agitated along the axis by gently tapping the sides of the platform (fig. 8). A MATLAB code was then used to quantify the

displacement of the graphite-mica sheets along each of the diagonal axes.

Figure 8: Setup of the high-speed camera for recording the lateral motion of a graphite piece.

C. *Finding the DLFC Spring Constant*

Another MATLAB code was used to fit the oscillations to the viscous damping model explained earlier in section II (fig. 9). Due to the high number of variables, fast Fourier transforms of the oscillations were required to find the approximate value of the DLSS natural damped frequency, w_d, as an initial value for the fit.

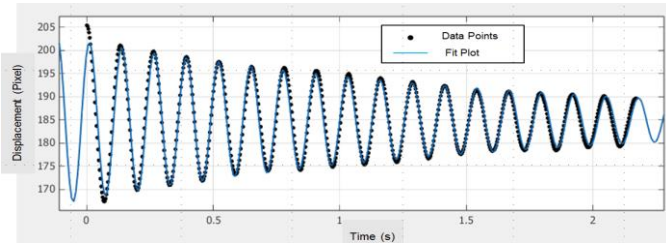

Figure 9: The fit of a graphite's oscillation.

IV. Designing and Producing Custom AFM Parts

There were initial attempts at modifying the designs of the specimen holder made by Dr. Qunyang Li by drilling circular indents for placing small metallic or boron silicate spheres to decrease the friction between parts. The attempts failed as it was difficult to make the indents equal depth, causing the specimen to be at an angle which leads to inaccurate measurements. The additional height from the spheres also rendered the existing screws unusable.

A complete redesign resulted in the entire specimen holder made up of aluminum metal instead of steel such that the magnets can be removed more easily. It consisted of three parts:

A. *Fixture*

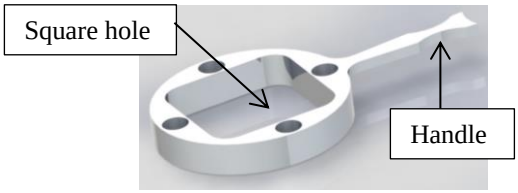

Figure 10: Rendering of the fixture.

The fixture (fig. 10) was designed to hold the magnets securely and enable easy removal when required without damaging them.

1) Square hole: It is a slip fit for the magnets.

2) Circular outline: When the handle of the fixture was pushed, the circular outline of the fixture enabled a concentric rotation, with the square hole ensuring the simultaneous rotation of the specimen.

3) Handle: The handle was specifically designed to align with the center axis of the diamagnetic levitation spring system for ease of maintaining a sense of the center axis' position while rotating the part.

4) Production process: Due to its small size, this part was the most challenging of the three parts to produce. The fixture was made from an aluminum stock. The conventional method of milling the stock down to the right thickness was by clamping the stock with a vice jaw. However, as the fixture was very thin, the large force from the vice jaw and the heat from the frictional forces of the milling caused the thin aluminum to bend and deform. A work-around was devised by sticking the back of the aluminum stock to the top surface of the vice jaw with a double sided tape. The surface of the vice jaw was cleaned beforehand with methanol to ensure maximum grip. This ensured that the aluminum stock will be at uniform thickness as there are no opposing horizontal pressures. However, this method was more inconsistent and slower than the conventional method. The large heat produced by the milling melted the double sided tape melting on numerous occasions, sending the aluminum stock flying in random directions. The stock will usually then be unusable and the process will have to start over again. As such, safety measures were taken including using higher amounts of coolant liquid, restricting access to the area surrounding the milling machine and greatly reducing the rate of milling.

After attaining the correct thickness of the aluminum stock, it was attached to another, thicker piece of stock using screws through the four small holes around the center square hole. This fixed the thin stock securely onto the vice jaw without it experiencing opposing horizontal forces from the vice jaw. A Computer Numerical Control (CNC) machine, the ProtoTRAK SMX was then used to mill the stock into a pre-programmed shape.

B. Holder

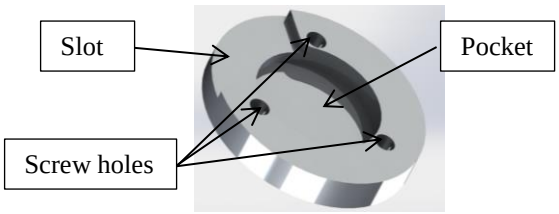

Figure 11: Rendering of the holder.

The holder (fig. 11) keeps the fixture secure in the setup. It was designed to have all the desirable features of the standard specimen holder with the addition of a mechanism for the rotation of the fixture.

1) Screw holes: The fixture is secured in position by three M2 screws which go through the three small holes. A tolerance of 0.254 mm in hole diameter was used as the machining allowance for possible errors in designing and manufacturing the holder. Given the minimum tolerance, the holder should not go out of position before it is secured with screws.

2) Slot: The fixture can be manipulated with its handle protruding through the slot. The maximum rotational angle (60^{o}) was only limited by the screw holes.

3) Pocket: The magnet's height was taken into account during the design of the holder by making a pocket. This ensured that the magnets would not interfere with the assembly.

4) Production process: The holder began as a rectangular aluminum stock. The three screw holes were first drilled into the stock. They were used to keep the stock in place while the ProtoTRAK SMX milled the remaining features such as the slot and pocket.

Figure 12: Assembly of Fixture and Handle

C. Cap

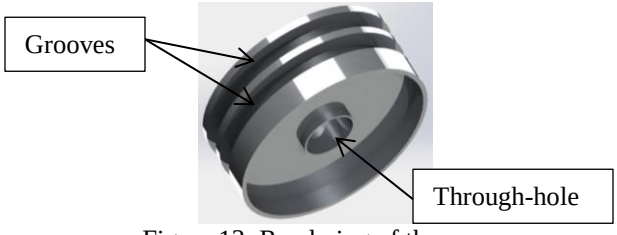

Figure 13: Rendering of the cap.

The third and final piece, the cap (fig. 13) was made because the graphite-mica sheet kept falling out from the DLSS during the positioning of the assembly in the UHV chamber. If the graphite-mica sheet falls down to the bottom of the chamber, much time would be required to retrieve the sheet.

1) Grooves: They are used for easy removal, introduction and storage of the cap within the UHV chamber by the manipulation fork (fig. 14). One groove will be used by the fork manipulator while the other groove is used to secure the cap in the storage space while the DLSS is being used for data collection. The gap between the grooves is made small to minimize the height profile of the cap. The grooves were modeled after the similar ones used for positioning the entire assembly.

2) Through-hole: It is used to view the graphite-mica sheet when the cap is placed on the assembly. This allows the user to know whether the graphite-mica sheet is in the correct position. The small indents at the bottom of the through hole forms encases the graphite-mica sheet, making sure that it will not slip out from the center of the magnets. In the rare event that the cap falls into the AFM pit, the cap can be hooked back up without requiring the opening of the bottom chambers.

3) Manufacturing: The cap is made by initially using a lathe to make the outer diameter and grooves. The ProtoTRAK SMX was then used to cut the inner diameters. Custom-made aluminum jaw clamps were required for the ProtoTRAK SMX to keep the cap in place without screws.

V. Collecting Data

After the DLSS is set up (fig. 15, 16), the cantilever tip was first lowered to the graphite-mica sheet manually, then automatically with feedback control through the AFM software. After the tip has approached, the direction of the cantilever is determined. If it is not aligned with the diagonal axis, it is moved a few micrometers upwards such that the DLSS can be realigned by carefully adjusting the handle. This procedure is repeated until an optimum orientation is achieved.

Figure 14: Manipulation fork.

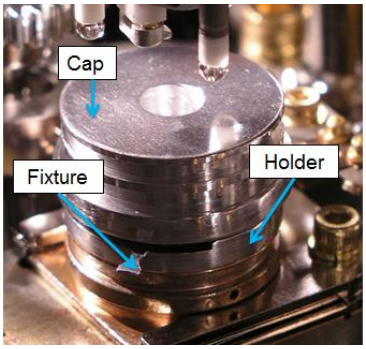

Figure 15: Complete assembly.

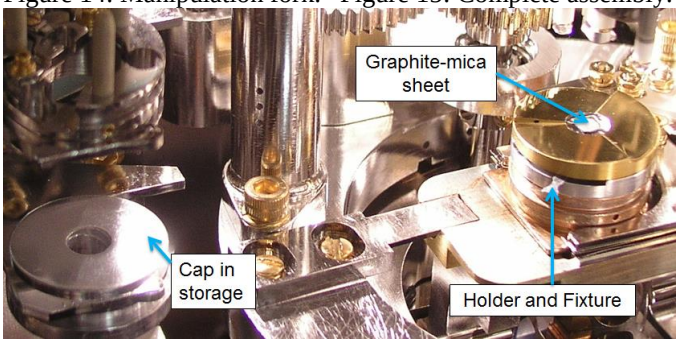

Figure 16: Setup just before collecting data.

The cantilever tip is then made to scan across a small surface area. The mica sheet and cantilever tip interface generates enough interfacial friction such that the tip drags the graphite-mica sheet laterally without relative sliding as it scans the area. The software records the signals along with the scan position of the cantilever tip. A relationship between the lateral voltage signal and the graphite-mica sheet's position is hence established.

The procedures above are used first when the DLSS is in ambient environment. Then, the vacuum chamber is sealed shut and air is removed until a high vacuum environment is achieved.

A MATLAB script is written to read the data file and perform the calculations as described in the background section of this paper.

VI. Results

A. Setup review

The DLSS and the assembly of parts including the custom parts worked as intended.

An interesting trait of the DLSS was noticed when the spring constant of different magnets and graphite-mica sheets were analyzed. The axis of the graphite-mica sheets was a determining factor of the oscillation's natural damped frequency, hence the spring constant of the sheets' displacement along the axis.

B. Lateral force constant

The calibration setup requires the user to manually adjust and approximate the position and alignment of the mica-graphite sheet using the handle. To take the variability and human error into account, the lateral force constant for a single setup is measured at various orientations (table 1).

Table 1: Lateral force constants of a setup at various orientations.

Orientation	α (10^{-2}μN/V)
Centered, aligned along an axis (ideal position).	7.15 ± 2.53
Cantilever displaced along x-direction.	8.79 ± 6.90
Cantilever displaced along y-direction.	9.46 ± 6.54
Graphite-mica sheet rotated several degrees using the handle.	9.04 ± 5.00

The lateral force constants have an average value of $8.61 \times 10^{-2}\mu N/V$ with a standard deviation of $0.873 \times 10^{-2}\mu N/V$. According to the previously used beam geometry method (Appendix), the theoretical lateral force constant value is $16.0 \times 10^{-2}\mu N/V$.

VII. Discussion and Conclusion

The assembly worked as intended, but the fixture's handle seemed too fragile and short. A thicker and longer handle will improve the durability and precision of the part.

The deviations in D-LFC results are acceptable given the wide range of orientations it was used in. The lateral force constant calculated using D-LFC agreed well with the beam geometry method as the beam geometry method's value was only 1.86 times the value calculated using the D-LFC. The error can be attributed to the idealized model of the beam geometry method. There are initial tests that indicate notable differences in lateral force constants determined in ambient atmosphere vs. vacuum. The D-LFC method needs to be investigated further with varying parameters such as atmosphere, scan size and speed. Work is also underway to compare both methods to other calibration techniques, such as the wedge calibration method.

Appendix

Beam geometry calibration method

The resonance frequency, f_0, of the silicon cantilever is found by taking the fast Fourier transform peak of the cantilever's thermal noise spectra.

The lateral stiffness of the cantilever, k_L, is calculated using the equation:

$$k_l = \frac{G * w * t^3}{3 * h^2 * l}$$

where G is silicon's shear modulus, w is the width of the cantilever also measured using optical microscopy, and h is the cantilever tip's height as provided by the manufacturer. The thickness, *t*, of the cantilever is calculated from:

$$t = 4 * \pi * f_0 * \left(\frac{l}{1.873}\right)^2 * \sqrt{\frac{3\rho}{E}} \quad [1]$$

where l is the cantilever's length as measured using optical microscopy, ρ is the density of silicon, and E is the Young's modulus of silicon. Note: The manufacturer's cantilever thickness value is not used due to its thin dimension being relatively small compared to its standard deviation and the stiffness is most strongly dependent on thickness. The cubic power of thickness in the lateral stiffness equation will result in any error in thickness exponentially increased in the calculated lateral stiffness.

Acknowledgement

The authors would like to acknowledge the financial support from the Littlejohn Undergraduate Research Program.

The authors would like to thank the Design and Prototyping Laboratory for providing access to tools and machines. We are also grateful for the motion tracking code provided by Boyang Qin from Prof. P. Arratia's lab; the high speed camera provided by Dr. Nicolad Jaumard from Prof. B. Weinstein's lab; the information provided by Dr. Qunyang Li and the advice given by Joe Valdez, Peter Rockett, and Peter Szczesniak.

We appreciate the help and support given by the Carpick group throughout the research.

References

[1] E. Meyer, H. J. Hug, and R. Bennewitz, Scanning Probe Microscopy: The Lab on a Tip, Springer-Verlag, Berlin, 2004.

[2] S.S. Barkley, Z. Deng, R. S. Gates, M. G. Reitsma, and R. J. Cannara, Rev. Sci. Instrum. 83, 023707 (2012).

[3] Q. Li, K. S. Kim, and A. Rydberg, Rev. Sci. Instrum. 77, 065105 (2006).